DOI: 10.1002/ejic.201100703

Zinc Complexes of Piperazinyl-Derived Aminephenolate Ligands: Synthesis, Characterization and Ring–Opening Polymerization Activity

Nduka Ikpo,[a] Lisa N. Saunders,[a] Jillian L. Walsh,[a] Jennifer M. B. Smith,[a] Louise N. Dawe,[b] and Francesca M. Kerton*[a]

Keywords: Ring-opening polymerization / Polymerization / Zinc / Carbon dioxide / Lactide / Caprolactone

A series of zinc complexes was prepared from 4,6-disubstituted (R,R′) *o*-[(4-methyl-1-piperazinyl)methyl]phenols ([ONN$^{R',R}$]H) and characterized by elemental analysis, ^{1}H and ^{13}C{^{1}H} NMR spectroscopy, and X-ray crystallography. Reaction of these products with diethylzinc gave Zn[ONN$^{t\mathrm{Bu},t\mathrm{Bu}}$]$_2$ (**1**) as a monometallic complex and {[μ-ONN$^{R',R}$]ZnEt}$_2$ [R′ = Me, R = *t*Bu, (**2**); R′ = R = *t*Bu (**3**); R′ = R = *t*Am (**4**)] bimetallic species that have distorted tetrahedral environments about the Zn centres. Reaction of **3** and **4** with alcohols gave {[ONN$^{t\mathrm{Am},t\mathrm{Am}}$]Zn(μ-OR′′)}$_2$ [R′′ = Bn (**5**); R′′ = Et (**6**)] bimetallic species in which the Zn centres are bridged by benzyl alkoxide and ethoxide groups, respectively. A morpholinyl derived ligand was also synthesized and characterized (**L4**H), and its 1:1 stoichiometric reaction with ZnEt$_2$ resulted in complex **7**, {[μ-ONO$^{t\mathrm{Bu},t\mathrm{Bu}}$]ZnEt}$_2$. The reactivity of complexes **2**–**7** in the ring-opening polymerization of *rac*-lactide (LA) and ε-caprolactone (ε-CL) was studied. Reactions of carbon dioxide with cyclohexene oxide in the presence of **6** or **7**/ROH (R = Bn, Et) afforded cyclohexene carbonate.

Introduction

Aminephenolate and related ligands that possess a mixed set of N- and O-donor atoms have attracted a great deal of interest over the past decade due to their ability to coordinate to a range of metal centres and the ease of systematic control of their steric properties by variation of their backbone and phenol substituents.[1–23] Various ligands of this type have been used in main group and early transition metal chemistry (including lithium,[2–3] magnesium,[4–10] calcium,[11] rare-earths,[12,13] zinc,[1,14–17,19] aluminium,[18,20] zirconium[21,22] and titanium[23]). Many of these complexes have been reported to be excellent initiators for the ring-opening polymerization (ROP) of cyclic esters such as LA. The quest is ongoing for new systems that can advance our understanding of this reaction, and ultimately lead to well controlled initiator performance in this and other polymerization reactions.

Recently, Issenhuth et al. reported the synthesis of cationic aluminium complexes supported by morpholine-derived aminephenolate ligands that act as efficient initiators for ROP of propylene oxide.[24] Of particular relevance to the current study, Carpentier and co-workers recently described the synthesis of zinc and magnesium complexes supported by ether-aminephenolate ligands, including those bearing morpholinyl side-arms, that are effective initiators for immortal ROP of cyclic esters.[25] Lappert and co-workers have reported zinc complexes stabilized by a piperazinylphenolate ligand,[26] and one such complex was found to uptake some CO_2 when cyclohexene oxide–CO_2 copolymerizations were attempted although no polymer product was isolated.

In this paper, we describe the synthesis and structural characterization of a group of piperazinyl–phenol ligands and a morpholinyl phenol ligand, their coordination chemistry with Zn, and their use as single and/or binary component initiators for the ROP of LA and ε-CL under various conditions, including under microwave (MW) irradiation. MW irradiation has not been used extensively in ROP of lactide facilitated by metal complexes.[27,28] In the two examples reported to date simple tin initiators, e.g. stannous octoate, were used and the resulting polymers have broad polydispersities. High reaction temperatures are normally detrimental to achieving controlled polymerization, however, MW methods allow rapid heating of reaction mixtures. Sluggish initiators, e.g. those bearing ligands with sterically demanding groups, normally require heating to enable a worthwhile reaction rate to be obtained. In such cases, MW heating may lead to a reduction in the number of side reactions e.g. transesterification by reducing the overall reaction time. Also, MW heating could lead to more rapid screening of potential ROP initiators.

[a] Department of Chemistry, Memorial University of Newfoundland,
St. John's, NL, A1B 3X7, Canada
Fax: +1-709-864-3702
E-mail: fkerton@mun.ca
[b] X-ray Crystallography Laboratory, Centre for Chemical Analysis, Research and Training, Memorial University of Newfoundland,
St. John's, NL, A1B 3X7, Canada
Supporting information for this article is available on the WWW under http://dx.doi.org/10.1002/ejic.201100703.

As many Zn phenolate and alkoxide complexes have shown good activity towards either copolymerization of CO_2 with epoxides or the formation of cyclic carbonates in this article we also describe our initial studies of the reactivity of **6** and **7**/ROH with carbon dioxide..[29,30]

Results and Discussion

The protio ligands were synthesized from the appropriate phenol, formaldehyde, and 1-methylpiperazine via a modified Mannich condensation reaction, as shown in Scheme 1. They were isolated in excellent yields. **L2H** has previously been prepared through a slightly different procedure that involved reduction with hydrobromic acid and neutralization with aqueous $NaHCO_3$,[26] however structural data for **L2H** have not been reported. The preparation of **L4H** through a Mannich condensation reaction in 1,4-dioxane under reflux has been reported previously.[25]

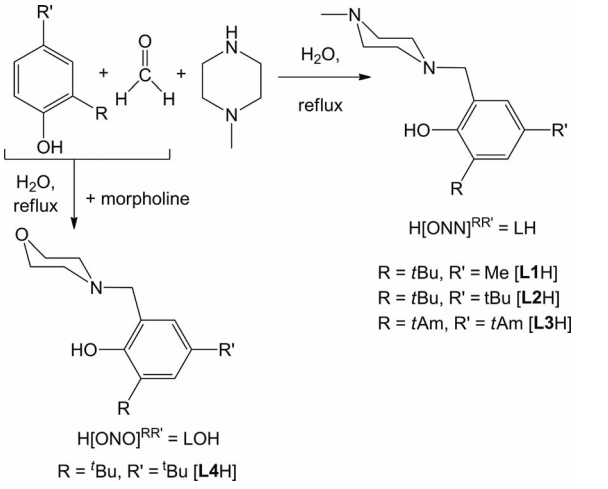

Scheme 1. Sythesis procedure for amine-phenolate ligand precursors.

The recently reported benign route (reaction in water)[31,31,32] to amine-phenol ligands reduces the amount of reagents required relative to more traditional reaction routes and afforded high yields of **L1H**–**L4H**. These were recrystallized from methanol (cooled to 0 °C). Their characterization by ^1H- and $^{13}C\{^1H\}$ NMR techniques afforded well resolved resonances for all proton and carbon environments, while elemental analyses showed that the compounds were obtained in pure form. Single crystals of **L2H** suitable for X-ray crystallography were grown via slow evaporation of a saturated methanol solution of **L2H** at ambient temperature. The solid state structure of **L2H** shown in Figure 1 and reveals intramolecular hydrogen bonding between the phenol and the proximal amine groups. The *N*-methylpiperazine ring adopts the normal chair conformation. Tables 5 and 6 summarize crystal data for all the structures reported in this article.

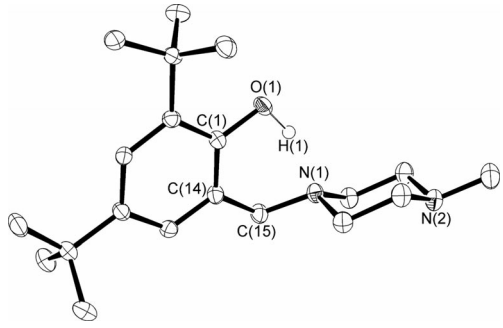

Figure 1. Molecular structure of **L2H**. The thermal ellipsoids are drawn at the 50% probability level; H1 atom included. Selected bond lengths [Å] and bond angles [°]: O(1)–C(1), 1.366(2); N(1)–C(15), 1.472(2); C(14)–C(15), 1.516(2); O(1)–C(1)–C(14), 119.73(14); O(1)–C(1)–C(2), 119.76(14); N(1)–C(15)–C(14), 113.72(14).

Synthesis and Characterization of Zinc Aminephenolate Complexes

Reactions of protio ligands $[ONN^{R,R'}]H$ with $ZnEt_2$ in toluene under ambient conditions led to the isolation of molecular zinc complexes $Zn[ONN^{tBu,tBu}]_2$ (**1**) and $\{[\mu\text{-}ONN^{R,R'}]ZnEt\}_2$ (**2–4**) in 56–96% yield (Scheme 2). Treatment of complexes **3** and **4** with two equivalents of benzyl alcohol and ethanol, respectively, in toluene at ambient

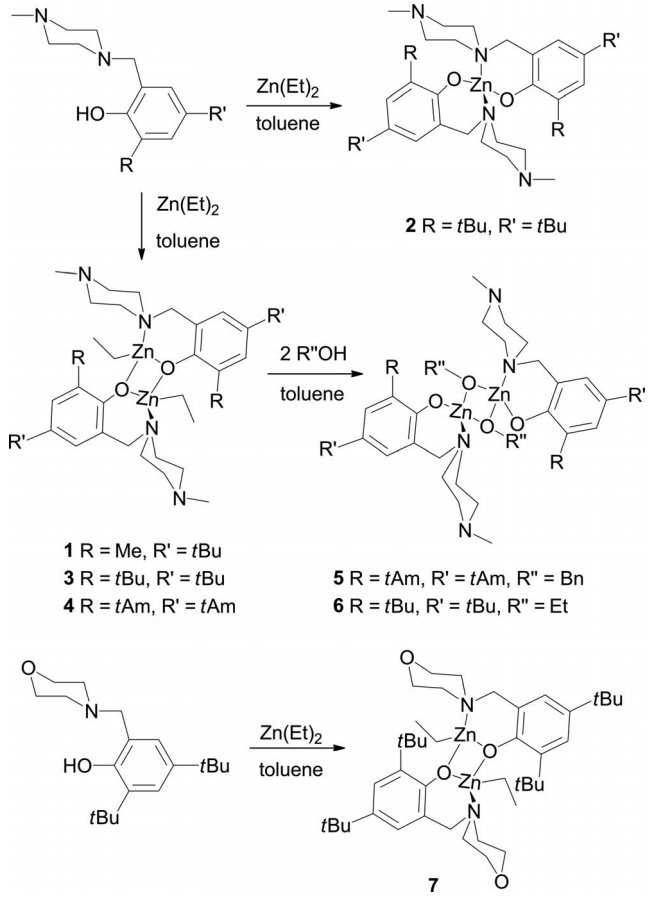

Scheme 2. Synthetic procedure for amine-phenolate zinc complexes.

temperature afforded **5** and **6**. An equimolar reaction between **L4**H and $ZnEt_2$ afforded $\{[\mu\text{-}ONO^{t\text{Bu},t\text{Bu}}]ZnEt\}_2$ (**7**) in 81% yield.

The synthesis of a monometallic zinc complex related to **1** has been reported by Lappert and co-workers, the synthesis proceeded via the indirect route of reacting a bimetallic phenolate-bridged ethylzinc complex with 2 equiv. of methanol.[26] Another similar monometallic zinc complex was reported by Sobota and co-workers, and was obtained from the reaction of 2 equiv. of an amine-phenol ligand with 1 equiv. of $ZnEt_2$.[33] In our case both the monometallic (**1**) and bimetallic (**2** and **4**) zinc complexes were synthesized by reaction of 1:1 ratio of $ZnEt_2$ with the corresponding ligands. Although all reactions were carried out under rigorous air- and moisture-free conditions, we cannot rule out the potential role of adventitious water in the preparation of **1**. In this regard, the preparation of **1** would proceed by a similar route to that reported by Lappert who used methanol as a proton source. Nevertheless, the reaction of **L2**H with an excess of $ZnEt_2$ in toluene did lead to the formation of the desired bimetallic zinc complex **2**. Treatment of complexes **3** and **4** with 2 equiv. of ethanol and benzyl alcohol, respectively, afforded alkoxy-bridged complexes **5** and **6**.

The zinc complexes **1**–**7** were characterized by elemental analyses, and ^1H and $^{13}C\{^1H\}$ NMR spectroscopy. The ^1H NMR spectra of **1**–**7** in C_5D_5N solvent recorded at room temperature showed broad resonances in the methylene ($PhCH_2N$) and amine methyl regions, which prompted variable-temperature NMR studies of the complexes. A portion of a representative variable-temperature spectrum of **4** is shown in Figure 2. At elevated temperature (343 K), sharp signals were discernable in the spectrum that were very informative for establishing the formation of the complexes **1**–**7**. The spectrum of complex **1** exhibits three sharp singlets associated with the aromatic and methylene protons, these signals occur at δ = 7.58, 7.11 and 4.07 ppm and are shifted from 7.26, 6.93 and 3.75 ppm where they are observed in the spectrum of free ligand (**L2**H). No Zn-ethyl resonances were observed in the spectrum of **1**. In contrast, the signals from the methylene ($PhCH_2N$) protons in **3** are observed at 3.65 ppm, and additional signals were observed at δ = 0.59 (quartet) and 1.57 ppm (triplet) that correspond to the ethyl group bound to the zinc ion. Similar resonances are observed in the spectra of complexes **2**, **4** and **7**. Upon lowering the temperature, the methylene signals became broader for all the complexes, which implied that at high temperature there is fast exchange on the NMR time scale of a coordinated pyridine or coordinated piperazine ligand and the free pyridine solvent. It should also be noted that in solution the bimetallic species (analogous to their solid state structures) are unlikely to exist in the presence of such a large quantity of Lewis base (C_5D_5N). However, use of this solvent was essential for gaining sufficient solubility for all samples studied, and to allow for direct comparison of their spectra.

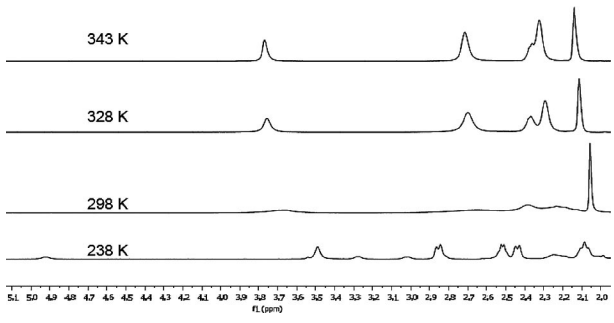

Figure 2. The methylene region of variable temperature ^1H NMR spectra of **4** in C_5D_5N.

X-ray Crystallographic Analyses of Zinc Complexes

Crystal structures of complexes **1**–**7** were determined by X-ray diffraction analysis. The molecular structure of complex **1** is shown in Figure 3 along with selected bond lengths and angles. The central zinc atom adopts a distorted tetrahedral coordination geometry and is coordinated by four donor atoms from two (methylpiperazinyl)phenolate ligands. The fact that one of the amine nitrogen atoms remains pendant can be attributed to the restriction of the chair conformation adopted by the piperazinyl unit of the ligand that orientates N(2) away from the central metal atom. Future studies will involve investigating the chemistry at this nitrogen centre. The structure of **1** is centrosymmetric (the zinc ion is located on a crystallographic inversion centre) with Zn–O and Zn–N distances within the normal ranges for related complexes. The more acute bond angles around Zn, O(1)–Zn(1)–N(1) 96.82(5)°, can most probably be associated with the bite of the six-membered C_3NZnO chelate ring. This ring adopts a legless chair[34] or slight sofa[1] conformation with the C(6) atom forming the backrest and situated ca. 0.76 Å out of Zn(1)–O(1)–C(20)–C(7)–N(1) plane.

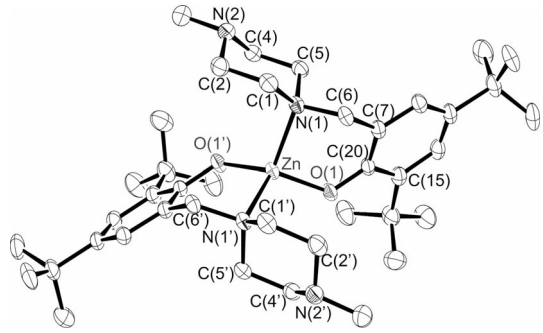

Figure 3. Molecular structure of **1**. The thermal ellipsoids are drawn at the 50% probability level; H atoms are excluded for clarity. The two halves of the molecule are symmetry related by inversion. Selected bond lengths [Å] and bond angles [°]: Zn(1)–O(1), 1.9008(11); Zn(1)–N(1), 2.1198(13); O(1)–C(20), 1.3357(17); N(1)–C(1), 1.4885(19); N(1)–C(5), 1.4909(19); N(1)–C(6), 1.4982(19); N(2)–C(2), 1.453(2); N(2)–C(3), 1.454(2); N(2)–C(4), 1.463(2); C(1)–C(2), 1.520(2); C(4)–C(5), 1.510(2); C(15)–C(20), 1.422(2); O(1)–Zn(1)–O(1), 124.94(7); O(1)–Zn(1)–N(1), 110.52(5); O(1)–Zn(1)–N(1′), 96.82(5); C(20)–O(1)–Zn(1), 125.45(10); C(1)–N(1)–C(6), 108.82(12); C(1)–N(1)–Zn(1), 114.91(9); C(6)–N(1)–Zn(1), 102.40(9); N(1)–C(1)–C(2), 111.18(13).

An ORTEP drawing of **2** is presented in Figure 4 along with selected bond lengths and angles. The structure exhibits a butterfly-like arrangement with the two ethyl groups positioned on the same side with respect to the Zn_2O_2 core plane, while the two piperazine units are situated on opposing sides of the Zn_2O_2 plane. This *cisoid* conformation of ethyl groups is rare in zinc ethyl chemistry, although another example has been reported.[35] Each zinc ion adopts a distorted tetrahedral coordination geometry consisting of two bridging phenolate oxygen atoms, one nitrogen donor and one ethyl group. The central metal ring, Zn_2O_2, displays a twisted geometry with O(1) and O(2) ca. 0.54 and 0.55 Å from the O(2)–Zn(1)–Zn(2) and O(1)–Zn(1)–Zn(2) planes, respectively. The angles at the central atoms Zn(1) [O(1)–Zn(1)–O(2), 80.47(8)°] and Zn(2) [O(1)–Zn(2)–O(2), 80.89(8)°] are narrower than the corresponding angles for the bridging oxygen atoms O(1) [Zn(2)–O(1)–Zn(1), 97.75(9)°] and O(2) [Zn(1)–O(2)–Zn(2), 96.55(9)°]. The acute angles are likely a result of the six-membered chelate ring that is enforced by the ligand. The two C_3OZnN chelate rings adopt boat conformations with C(6) and O(1) ca. 0.62 and 0.71 Å from the Zn(1)–C(17)–C(7)–N(1) plane, while C(23) and O(2) are ca. 0.64 and 0.74 Å from the Zn(2)–C(34)–C(24)–N(2) plane. The Zn–C bond lengths in **2** are comparable to those in related complexes reported in the literature,[36] where the mean Zn–C bond lengths in such species are 1.978 Å. Within those complexes that are bimetallic, the ethyl groups are transoidal.[21,37,38] The Zn–O bond lengths in **2** are similar to the mean distance [2.039 Å] determined from a literature survey, and are comparable to those within related zinc complexes that are reported in the literature.[26,35,38–41] The Zn(1)–Zn(2) distance [3.0527(6) Å] is close to that reported by Gibson [3.0276(5) Å], while the O(1)–O(2) separation distance [2.634 Å] is shorter [2.817(3) Å].[1]

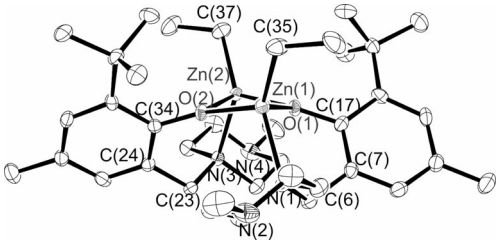

Figure 4. Molecular structure of **2**. The thermal ellipsoids are drawn at the 50% probability level; H atoms are excluded for clarity. Selected bond lengths [Å] and bond angles [°]: Zn(1)–C(35), 1.981(3); Zn(1)–O(1), 2.037(2); Zn(1)–O(2), 2.043(2); Zn(1)–N(1), 2.148(3); Zn(1)–Zn(2), 3.0527(6); Zn(2)–C(37), 1.991(3); Zn(2)–O(1), 2.015(2); Zn(2)–O(2), 2.047(2); Zn(2)–N(3), 2.143(3); O(1)–C(17), 1.361(3); O(2)–C(34), 1.353(3); C(35)–Zn(1)–O(1), 117.75(13); C(35)–Zn(1)–O(2), 124.72(12); C(35)–Zn(1)–N(1), 123.31(12); O(1)–Zn(1)–N(1), 93.77(9); O(2)–Zn(1)–N(1), 105.03(9); C(37)–Zn(2)–O(1), 123.41(12); C(37)–Zn(2)–O(2), 115.93(12); O(1)–Zn(2)–O(2), 80.89(8); Zn(2)–O(1)–Zn(1), 97.75(9); Zn(1)–O(2)–Zn(2), 96.55(9).

The single crystal structure of complex **3** depicted in Figure 5 reveals a centrosymmetric bimetallic complex with the zinc centres bridged through the oxygen atoms of the phenolate ligands. The coordination geometry at the zinc atom is a distorted tetrahedron. It should be noted that the bond angle O(1)–Zn(1)–O(1′) [83.78(13)°] is wider than that in Bochmann's $[EtZn(\mu\text{-}OC_6F_5)(py)]_2$ (py = pyridine) complex [78.00(5)°], which contains a *trans*-alkylzinc centre with a phenolate ligand and a nitrogen donor (in this case from pyridine).[42] The similarities in the types of donors in the coordination spheres of Zn in each complex allows the difference in the bond angles to be attributed to the chelate bite angle of **L2** in complex **3**, whereas the donors in Bochmann's complex are not linked and are free to orientate themselves with minimal constraint. In **3**, C(15) and O(1) lie ca. 0.75 and 0.45 Å from the Zn(1)–N(1)–C(6)–C(1) mean plane, inducing the chelate ring to adopt a chair conformation, while the zinc atoms lie ca. 0.58 Å above the plane defined by the coordinated N(1), C(21) and O(1) atoms. The central Zn_2O_2 ring is planar with the angle at Zn(1) being narrower than that at O(1). The Zn–C, Zn–N and Zn–O bond lengths are within the ranges previously reported for zinc complexes.[1,26,39,43] The ethyl groups on each of the two metal centres lie *trans* to each other. Presumably, the large *tert*-butyl group in the 4-position of the phenolate donor in **3**, although distant from the metal coordination sphere, causes the ethyl groups to orientate themselves in a *trans* arrangement in contrast to the *syn-cis* arrangement in **2**, in which the 4-position of the phenolate ligand is occupied by a methyl group.

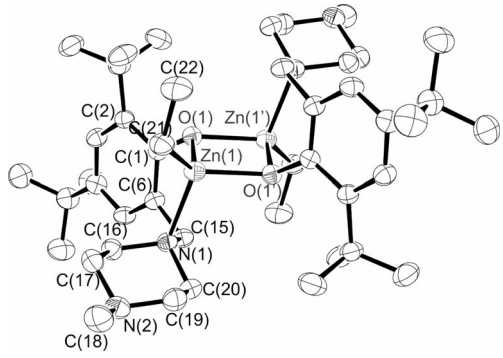

Figure 5. Molecular structure of **3**. The thermal ellipsoids are drawn at the 50% probability level; H atoms are excluded for clarity. The two halves of the molecule are symmetry related by inversion. Selected bond lengths [Å] and bond angles [°]: Zn(1)–C(21), 1.977(4); Zn(1)–O(1), 2.052(3); Zn(1)–N(1), 2.185(4); Zn(1)–Zn(1), 3.068(5); O(1)–C(1), 1.362(3); N(1)–C(20), 1.479(4); N(1)–C(16), 1.483(4); N(1)–C(15), 1.498(4); N(2)–C(17), 1.457(4); N(2)–C(18), 1.458(4); N(2)–C(19), 1.460(4); C(1)–C(2), 1.416(4); C(21)–Zn(1)–O(1), 124.87(11); O(1)–Zn(1)–O(1′), 83.78(13); C(21)–Zn(1)–N(1), 118.53(16); O(1)–Zn(1)–N(1), 92.53(10); O(1)–Zn(1)–N(1′), 103.06(11); C(1)–O(1)–Zn(1), 117.95(18); C(1)–O(1)–Zn(1′), 123.86(17); Zn(1)–O(1)–Zn(1′), 96.22(13); C(20)–N(1)–C(16), 106.4(2); C(20)–N(10)–C(15), 107.5(2); C(16)–N(1)–C(15), 110.1(2); C(20)–N(1)–Zn(1), 113.99(18); C(16)–N(1)–Zn(1), 114.17(18).

The single-crystal X-ray data for **4** were of poor quality due to merohedral twinning of the crystals and their weak diffraction, however the structure and connectivity of **4** was

confirmed and authenticates the theory that it is structurally analogous to **3**. A ball and stick model of **4** is available in the Supporting Information.

Reaction of the alkyl complexes with alcohols afforded alkoxy-bridged complexes. Suitable single crystals of these complexes were grown by the slow evaporation of a hexane/toluene mixture (**5**) and from a saturated toluene solution at –35 °C (**6**). The molecular structures of **5** and **6** reveal the bimetallic nature of these species. An ORTEP drawing of **6** is shown in Figure 6 and an illustration of the structure of **5** is available in the Supporting Information. The zinc centres in these complexes adopt distorted tetrahedral geometries and are bridged by the oxygen atoms of the ethoxide or benzyl alkoxide groups to form planar Zn_2O_2 cores. Comparison of the angles within the Zn_2O_2 planar cores of complexes **5** and **6** reveals that the O–Zn–O bond angle in **6** is slightly narrower than that in complex **5**, while the Zn–O–Zn bond angle is wider in complex **6** than in complex **5**. The bond lengths within the two complexes are similar, and **6** contains bond lengths comparable to those in a related ethoxide-bridged zinc species.[44]

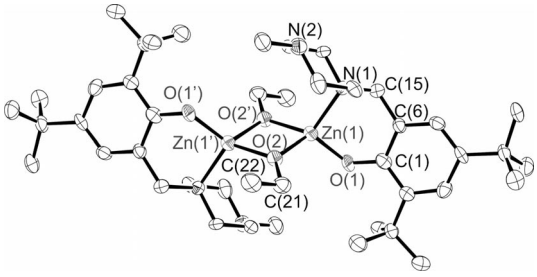

Figure 6. Molecular structure of **6**. The thermal ellipsoids are drawn at the 50% probability level; H atoms are excluded for clarity. Selected bond lengths [Å] and bond angles [°]: Zn(1)–N(1), 2.088(6); Zn(1)–Zn(1), 2.954(2); O(1)–C(1), 1.330(8); O(2)–C(21), 1.404(8); O(2)–Zn(1), 1.957(5); O(2) –Zn1–O(2), 82.0(2); O(1)–Zn(1)–N(1), 100.8(2); O(2)–Zn(1)–N(1), 117.4(2); C(21)–O(2)–Zn(1), 131.9(4); Zn(1)–O(2)–Zn(1′), 98.0(2).

Crystals of complex **7** were obtained by cooling a saturated toluene solution to –35 °C. The solid state structure of complex **7** (Figure 7), like the related piperazinyl complex **3**, contains zinc atoms coordinated by the phenolate oxygen atom and the proximal nitrogen atom of the ligand to form a planar Zn_2O_2 core. The bond angles and distances are in the range known for bimetallic zinc phenolate complexes, and comparable to those in **3**.[1,26,39,43]

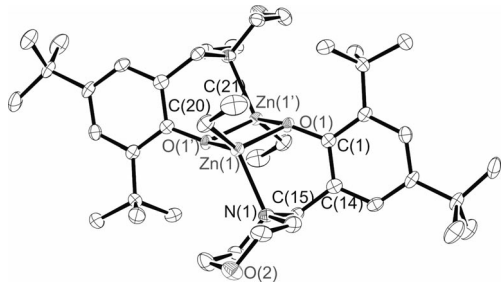

Figure 7. Molecular structure of **7**. The thermal ellipsoids are drawn at the 50% probability level; H atoms are excluded for clarity. The two halves of the molecule are symmetry related by inversion. Selected bond lengths [Å] and bond angles [°]: Zn(1)–C(20), 1.956(6); Zn(1)–O(1), 2.071(4); Zn(1)–N(1), 2.177(5); Zn(1)–Zn(1), 3.0608(14); O(1)–C(1), 1.354(7); O(2)–C(17), 1.393(8); C(20)–Zn(1)–O(1), 128.8(2); C(20)–Zn(1)–O(1′), 115.6(2); O(1)–Zn(1)–O(1), 82.87(17); C(20)–Zn(1)–N(1), 121.1(2); O(1)–Zn(1)–N(1), 92.70(18); C(1)–O(1)–Zn(1), 119.1(3).

Polymerization of Cyclic Esters

Ring-Opening Polymerization of rac-Lactide

The activities of complexes **2**–**5** and **7** as initiators for ROP of LA in toluene (Table 1 and Figure 8) and neat ester (Table 2) were examined. Compound **7** has been studied previously by Carpentier and co-workers.[25] It is included here for comparative purposes and afforded a polymer with relatively narrow M_w/M_n (M_w = weight averaged molecular weight, M_n = number average molecular weight). For the

Table 1. Details of the ring-opening polymerizations of LA initiated by complexes **2**–**5** and **7** in toluene.

Entry	Initiator	$[LA]_0:[Zn]_0:[ROH]_0$	t [min]	T [°C]	Conv. [%][d]	M_{ncal}[e] × 10^3	M_n[f] × 10^3	M_w/M_n[f]	P_r[g]
1	2	100:1:1[a]	60	60	97.1	13.9	10.9	1.25	0.49
2	2	100:1:1[a]	10	60	96.0	13.8	7.99	1.23	0.49
3	2	200:1:1[a]	15	60	96.3	27.7	11.8	1.39	0.53
4	3	100:1:1[a]	90	70	98.0	14.1	13.6	1.32	0.45
5	3	100:1:1[b]	120	70	96.4	13.9	12.0	1.60	0.53
6	3	100:1:0	120	70	0.1	–	–	–	–
7	3	200:1:1[b]	120	70	98.0	28.2	13.3	1.76	0.55
8	3	300:1:1[b]	120	70	98.3	42.5	15.3	1.87	0.49
9	3	100:1:1[b]	5	120[c]	90.0	12.9	12.0	1.33	0.47
10	3	100:1:1[a]	5	120[c]	93.6	13.5	9.19	1.42	0.47
11	4	100:1:1[a]	60	70	97.0	11.4	12.3	1.42	0.51
12	5	100:1:0	15	70	94.9	13.7	10.0	1.37	0.47
13	7	100:1:1[a]	30	60	97.6	13.9	9.56	1.25	0.49

[a] In the presence of one equivalent of benzyl alcohol. [b] In the presence of one equivalent of *tert*-butyl alcohol. [c] Microwave reaction (MW). [d] Determined by ^{1}H NMR spectroscopy. [e] The M_{ncal} value of the polymer was calculated with M_{ncal} = ([*rac*-LA]$_0$/[Zn]$_0$) × 144.13 × conv. %/100. [f] The M_n value was calculated according to $M_n = 0.58 M_{nGPC}$, where M_{nGPC} is the value of Mn determined by GPC (chloroform) and is relative to polystyrene standards. [g] P_r is the probability of racemic enchainment of the monomers units, as determined by homodecoupled ^{1}H NMR spectroscopy according to the method reported by Coates et al.[51]

Table 2. Details of the bulk polymerizations of LA initiated by complexes **5** and **6** and preformed at 130 °C.

Entry	Initiator	$[LA]_0:[I]_0$	t [min]	Conv. [%][a]	M_{ncal}[b] $\times 10^3$	M_n[c] $\times 10^3$	M_w/M_n[c]	P_r[d]
1	**5**	100:1	15	54.8	7.90	10.8	1.39	0.53
2	**5**	100:1	60	74	10.7	12.7	1.67	0.53
3	**5**	100:1	120	91.1	13.2	20.2	1.65	0.51
4	**6**	100:1	15	41.4	4.72	1.28	1.18	0.53
5	**6**	100:1	60	83.9	9.58	3.39	1.54	0.53
6	**6**	100:1	120	95.2	10.9	3.96	1.66	0.53

[a] Determined by ^{1}H NMR spectroscopy. [b] The M_{ncal} value of the polymer was calculated with $M_n = ([LA]_0/[Zn]_0) \times 144.13 \times$ conversion %/100. [c] The M_n value was calculated according to $M_n = 0.58 M_n^{GPC}$, where M_n^{GPC} is the value of M_n determined by GPC (chloroform) and is relative to polystyrene standards. [d] P_r is the probability of racemic enchainment of monomers units, as determined by homodecoupled ^{1}H NMR spectroscopy according to the method reported by Coates et al.[51]

piperazinyl-derived initiators, M_w/M_n values for polylactide (PLA) were between 1.25 and 1.87. Reaction rates generally correlated with both the steric demands of the ligand and coinitiator (alcohol), with **2** and BnOH affording near quantitative conversions within shorter times than its *t*Am and *t*Bu analogues, and with activity comparable to that of compound **7**. Overall the *M*n values of the polymer samples were lower than the expected values based on % conversion. This deviation likely implies that some transesterification reactions and/or a slow initiation step relative to propagation occurred. Both the broadening of the molecular weight distribution and the deviation from expected M_n increased with increasing $[LA]_0:[Zn]_0$ ratio (Table 1, entries 2 and 3, entries 6–8), and with increasing reaction time and temperature. These trends are frequently observed in ROP of cyclic esters.[45–47] In an attempt to distinguish between less controlled polymerization due to slow initiation vs. transesterification, the single component initiator **5** was studied (Table 1, entry 12). The M_w/M_n for the resulting polymer was not significantly different to that obtained for PLA with **4**/BnOH under similar conditions(Table 1, entry 11). However, as expected, **5** did result in more rapid polymerization than **4**/BnOH. The difference in the rate of polymerization could be attributed to the time lapse required for the transformation of the precursor alkyl species, by alcoholysis, to the active alkoxide complex.

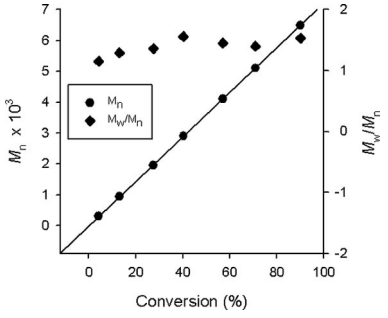

Figure 8. Plots of M_n and PDI (PDI = M_w/M_n and is determined by GPC) vs. monomer conversion for **3**/*t*BuOH initiated ROP of LA. Conditions: [LA]:[Zn]:[*t*BuOH] = 50:1:1, $[Zn]_0$ = 18.2 mM, toluene, 60 °C, 0.1 mL aliquots taken at the given intervals. Diamonds correspond to M_w/M_n and circles to M_n.

For the Zn-alkyl species the presence of alcohol was necessary to generate an efficient initiator system for the polymerization of LA, as has been reported in the literature.[48–49] The use of BnOH and *t*BuOH as coinitiators with **3** was studied in reactions conducted with conventional heating and MW irradiation. It was noted that conversions of 90% and 93% could be reached in 5 min with MW for *t*BuOH and BnOH, respectively (Table 1, entries 9 and 10), but similar conversions with conventional heating required significantly longer reaction times, particularly for *t*BuOH when compared with BnOH (Table 1, entries 4 and 5). The M_n of the PLA prepared via a MW method showed good agreement with the theoretical values. These data imply that MW irradiation can be used to assist in the control of ROP when bulky coinitiators are used, as there is a smaller apparent difference in the initial reaction rate under such conditions compared with conventional heating methods. This could be useful particularly in the preparation of star-polymers and other systems where a sterically congested coinitiator is required. It should be noted that in the conventionally heated reactions, solutions of monomer and initiator were heated separately and then mixed once the desired reaction temperature was achieved.

Microstructural analyses of the resulting PLA were performed through inspection of the methine region of the homodecoupled ^{1}H NMR spectra. P_r values (probability of racemic enchainment of the monomer units) were generally close to 0.5 indicating that an atactic polymer was produced. Reactions with good initiation rates (Table 1, entries 4, 9, 10 and 12) afforded polymers with a very slight isotactic bias (P_r = 0.45–0.47) whereas long reaction times and high temperatures (excluding MW reactions) gave polymers with a very slight heterotactic bias (P_r = 0.51–0.55). The latter polymers had, on average, broader molecular weight distributions than those with $P_r < 0.5$. Therefore, the apparent increase in heterotacticity is likely to be an artefact of transesterification reactions, and the small degree of isotacticity is probably induced through a chain-end control mechanism. Occurrence of transesterification was confirmed by matrix-assisted laser desorption ionisation time-of-flight mass spectrometry (MALDI-TOF MS) and ^{1}H NMR end-group analysis of the polymers. In the mass spectra, two main series of signals were observed that were separated by a difference of 72 in *m*/*z*. These were assigned to open chain (even mass) polymers and oligomers clustered with Na^+ and K^+ ions. Two less intense series of signals (80% less intense than the main series signals), separated by 72 in *m*/*z*, were also observed. These weaker signals were

assigned to cyclic (odd mass) polymers and oligomers clustered with Na^+ and K^+ ions. ^1H NMR spectra of the polymers reported in this paper all contained resonances attributable to OH end groups. However, integration of either the –OH or RO– end group resonances relative to the methine protons generally afforded higher molecular weights than those obtained through either gel permeation chromatography (GPC) or MALDI-TOF MS analysis, the values were up to three times higher for polymers with the broadest M_w/M_n values. Therefore, the ^1H NMR end group analyses confirmed that intramolecular transesterification had occurred, which produced cyclic species and led to less intense end group resonances than predicted based on the M_n data. Our results contrast with the previously reported work of Carpentier and coworkers where no transesterification was apparent (as indicated by narrower molecular weight distributions than seen for our polymers and by MALDI-TOF MS studies) and a heterotactic bias was observed in the resulting polymers (P_r = 0.60)[25] although to achieve this THF was used as the solvent, while in toluene a slight isotactic bias was observed (P_r = 0.46), in line with our results obtained with piperazinyl systems. For the single morpholinyl derived initiator in our study, we found P_r = 0.49 for the PLA formed in toluene (Table 1, entry 13). The first-order plot for solution polymerization with this initiator (Figure 9) was linear with k_{app} = 0.263 min^{-1}. The rates observed for the piperazinyl-derived species in this study were between 0.010 and 0.030 min^{-1}, both in toluene and in molten LA. These data suggest that the morpholinyl derived systems are superior initiators when compared with their piperazinyl analogues in terms of fast reaction rates and greater degree of control. We propose that the outer sphere ether group in these systems may play a role in directing the incoming monomer for reaction at the metal centre, and that the outer sphere tertiary amine group is less efficient in this process.

ROP reactions with the single component initiators **5** and **6** were also performed under solventless conditions at 130 °C, Table 2. Conversions reached more than 90% over 2 h (Table 2, entries 1 and 6) suggesting slow initiation compared with analogous solution phase polymerizations. The first-order plots for the bulk polymerization of LA with **5** and **6** as initiators (Figure S7) were linear with k_{app} values

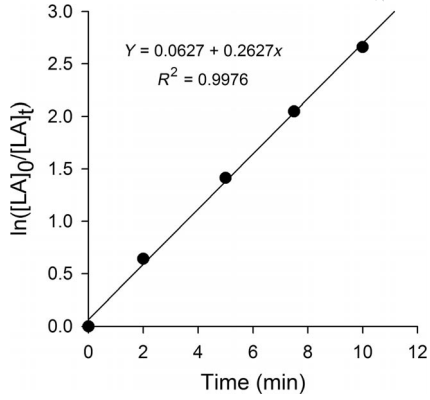

Figure 9. First-order plot of LA consumption in a reaction with **7**/BnOH conducted at 60 °C. Conditions: [LA]:[Zn]:[ROH] = 100:1:1, 10 mL of toluene, $[Zn]_0$ = 32.0 mM.

of 0.0179 and 0.0247 min^{-1}, respectively. Bulk polymerization of LA in the presence of **6** (an ethoxide complex) is moderately faster than in the presence of **5** (a benzyl alkoxide species) due to the differences in the steric demands of the initiating alkoxide ligands. Complex **5** afforded higher molecular weight polymers than **6**. The M_n values of these polymers were also significantly higher than the predicted values (M_{ncal}), which might be attributed to decomposition of the initiators at the high temperatures required for melt polymerization. Initiator decomposition leading to higher than expected M_n values has been observed previously by Drouin et al.[50] Both systems afforded predominantly atactic polymers under these reaction conditions due to the high temperatures used.

Ring-Opening Polymerization of ε-Caprolactone

Polymerization of ε-CL by complexes **2**–**5** and **7** was also assessed (Table 3). Similar trends in behaviour can be seen in the results from these reactions when compared to those of the ROP of LA study, e.g. slow initiation and reaction rates when *t*BuOH was used as the coinitiator (Table 3, entries 3 and 4). Molecular weight distributions were between 1.22 and 1.82. Conversions were generally higher when BnOH, which is less sterically demanding, was used in place of *tert*-butyl alcohol. Of the complexes studied those containing the *t*Am substituted ligands afforded initiators with

Table 3. Details of the ring-opening polymerizations of ε-CL initiated by complexes **2**–**5** and **7** in toluene.

Entry	Initiator	$[\varepsilon\text{-CL}]_0$:$[Zn]_0$:$[ROH]_0$	*t* [min]	*T* [°C]	Conv. [%][d]	M_{ncal}[e] × 10^3	M_n[f] × 10^3	M_w/M_n[f]
1	**2**	100:1:1[b]	15	60	74.4	8.49	5.69	1.27
2	**2**	200:1:1[b]	60	60	94.5	21.4	9.72	1.34
3	**3**	100:1:1[a]	120	70	17.1	–	–	–
4	**3**	200:1:1[a]	270	70	76.3	17.4	14.6	1.82
5	**3**	100:1:1[a]	5	130[c]	50.0	5.71	12.2	1.37
6	**3**	100:1:1[b]	5	130[c]	98.3	11.2	7.70	1.46
7	**4**	100:1:1[b]	40	70	99	11.3	8.56	1.22
8	**5**	100:1:0	60	70	95	10.8	9.03	1.30
9	**7**	100:1:1[b]	30	70	88.5	20.2	17.5	1.21

[a] In the presence of one equivalent of *tert*-butyl alcohol. [b] In the presence of one equivalent of benzyl alcohol. [c] Microwave reaction (MW). [d] Determined by ^1H NMR spectroscopy. [e] The M_{ncal} value of the polymer was calculated with M_n^{cal} = ($[\varepsilon\text{-CL}]_0/[Zn]_0$) × 114.14 × conv. %/100. [f] The M_n value was calculated according to $M_n = 0.56 M_n^{GPC}$, where M_n^{GPC} was determined by GPC (chloroform), and is relative to polystyrene standards.

Table 4. Details of the reactions of cyclohexene oxide (CHO) with CO_2 in the presence of Zn complexes and co-catalysts.

Entry	Catalyst	Cocatalyst	$[CHO]_0$:$[Zn]_0$:$[Co\text{-}cat]_0$	t [h]	P [bar]	T [°C]	Conv. [%][a]
1	–	Bu_4NBr	500:0:1	24	65	100	39.0 (100% *cis*)
2	**6**	–	500:1:0	18	45	70	0
3	**6**	DMAP	500:1:1	16	45	70	0
4	**6**	Bu_4NBr	500:1:1	18	45	70	4.8
5	**6**	Bu_4NBr	500:1:1	24	65	100	57.1 (96.2% *cis*)
6	**7** + BnOH	Bu_4NBr	500:1:1	18	45	70	8.3
7	**7** + EtOH	Bu_4NBr	500:1:1	24	65	100	45.1 (86.4% *cis*)

[a] Determined by the relative intensities of the methine protons in the ^1H NMR spectra.[58]

the greatest degree of reaction control for ROP of ε-CL, in that **4** and **5** afforded ε-polycaprolactone [P(ε-CL)] with narrow molecular weight distributions and molecular weights close to the expected values (Table 3, entries 7 and 8). First-order plots of the consumption of ε-CL in ROP reactions conducted at 70 °C in the presence of **7**/BnOH and **2**/BnOH are shown in Figure 10.

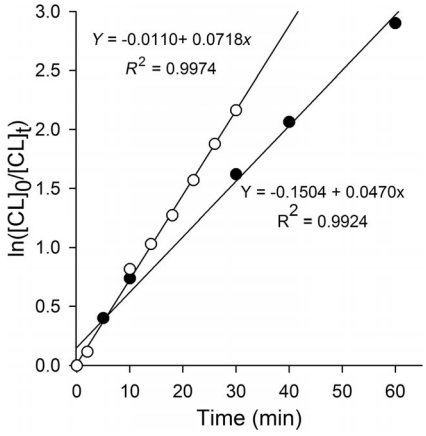

Figure 10. First-order plots of ε-CL consumption in ROP reactions conducted at 70 °C with **7**/BnOH (hollow circles) and **2**/BnOH (filled circles). Conditions: [ε-CL]:[Zn] = 200:1, 1 equiv. BnOH, $[Zn]_0$ = 22.5 mM (**7**) and 18.8 mM (**2**).

Reactivity of Complexes Towards CO_2 and Cyclohexene Oxide Coupling

Amongst catalytic coordination complexes for CO_2/epoxide couplings and copolymerizations, zinc is central to many of the species studied.[29,30,52–55] Therefore, studies were performed with **6** and **7**/ROH, with 4-(dimethylamino)-pyridine (DMAP) and Bu_4NBr as cocatalysts (Table 4), to evaluate their activities in the reaction of CO_2 with cyclohexene oxide. A control reaction was performed with Bu_4NBr alone as ionic salts such as this are known to catalyze the formation of cyclic carbonates (Table 4, entry 1).[56–57] Compounds **6** and **7** exhibit some activity towards cyclic carbonate formation under high temperature and pressure conditions and in the presence of an ionic cocatalyst. Comparison of entries 1 and 5 (Table 4) indicates that the zinc complex does play a role in this reaction as the conversion increases by 18.1% when it is present in the reaction mixture, and a small amount of *trans*-cyclic carbonate was observed. A **7**/EtOH/Bu_4NBr combination under the same conditions, entry 7, produced slightly less carbonate but with a larger amount of the *trans*-isomer than when only Bu_4NBr is present in the reaction mixture. The *cis*- and *trans*-isomers are likely formed through different mechanisms, with the *trans*-isomer probably formed through a back-biting reaction at the metal centre. Although conversions were modest and high temperatures and pressures were required, compared to state-of-the-art catalysts reported in the literature these results can act as a starting point for further studies, and also give some indication as to the reason for CO_2 uptake by the related Zn complexes reported by Lappert and co-workers.[26]

Conclusions

Piperazinyl-derived amine-phenolate protio ligands can be prepared in excellent yields in water via a modified Mannich condensation reaction. As expected, these ligands readily react with diethylzinc and generally afford phenolate bridged Zn-Et dimers. These complexes readily undergo alcoholysis to yield alkoxide bridged species. A range of these complexes has been structurally characterized. The Zn-Et species in the presence of an alcohol, and the alkoxide complexes as single component initiators, are able to facilitate ring-opening polymerization of cyclic esters, however, no control of stereoselectivity is observed in ROP of LA and this is probably due to the solvent employed in these reactions. In comparison with morpholinyl derived complexes, the piperazinyl-derived species show slower ROP reaction rates. MW irradiation was used in some of the ROP reactions and was useful in reducing reaction times whilst maintaining control of the reaction (i.e. increased polydispersities that are usually due to the high temperatures used in ROP reactions were not observed). Both classes of complex show slight activity towards cyclic carbonate formation involving cyclohexene oxide and carbon dioxide. These studies suggest that an outer sphere ligand group or base (ether or amine) within an initiating or catalytic species can affect the outcome of ROP and potentially other reactions. Further studies utilizing these interesting ligands are underway in our laboratory.

Experimental Section

General Considerations: All experiments involving metal complexes were performed in a nitrogen atmosphere with standard Schlenk and glovebox techniques. THF was distilled under nitrogen over sodium/benzophenone. Toluene and hexane were purified by an MBraun Solvent Purification System. Deuterated solvents (C_6D_6, $CDCl_3$, C_5D_5N) were purchased from Cambridge Isotope Laboratories, Inc. and purified and dried before use. All solvents were degassed by freeze-vacuum-thaw cycles prior to use. 2,4-bis(*tert*-butyl)phenol, 2-*tert*-butyl-4-methylphenol, 2,4-bis(*tert*-amyl)phenol, *n*-butyllithium, 1-methyl piperazine, morpholine, diethylzinc (15 wt.-% solution in hexane), LA, ε-CL and cyclohexene oxide were purchased from Sigma–Aldrich or Alfa Aesar. Monomers were dried and degassed prior to use. Elemental analyses were performed by Canadian Microanalytical Service Ltd., Delta, BC, Canada. ^{1}H and ^{13}C{^{1}H} NMR spectra were recorded on a Bruker Avance 500 MHz spectrometer at 25 °C (unless otherwise stated) and were referenced internally with respect to the residual proton and ^{13}C resonances of the solvent. ^{13}C signals were assigned by heteronuclear single quantum correlation spectroscopy (HSQC) experiments. MALDI-TOF MS measurements were performed with an Applied Biosystems Voyager DE-PRO equipped with a reflectron, delayed ion extraction and high performance nitrogen laser (337 nm). Anthracene was the matrix for the ligands and complexes.[59–60] Mass spectra were also obtained by atmospheric pressure chemical ionization mass spectrometry (AP-CI MS) in positive mode (70 eV) with an Agilent 1100 LC mass spectrometer. GPC data were collected on a Viscotek GPCMax System equipped with a Refractive Index Detector, and columns were purchased from Phenomenex (Phenogel 5 μ Linear/mixed bed 300 × 4.60 mm column in series with a Phenogel 5 μ, 100 Å, 300 × 4.60 mm column). Samples were run in chloroform at a concentration of 1 mg/mL, and at 35 °C. The instrument was calibrated against polystyrene standards (Viscotek) to determine the molecular weights (M_n and M_w) and the polydispersity index (M_w/M_n) of the polymers. For PLA samples, P_r was determined by analysis of the methine region of the homonuclear decoupled ^{1}H NMR spectra ($CDCl_3$). The equations used to calculate P_r were as described by Coates et al.[51] The conversions were determined by integration of the relative intensities of the OC*H*Me resonances corresponding to the residual LA and poly(*rac*-lactide), and integration of the ε-methylene signals due to the residual ε-CL and poly(ε-caprolactone).

Microwave heated polymerizations were performed with a Biotage Initiator™ eight microwave synthesizer.

Crystallographic Procedures: All crystals were mounted with paratone oil onto a low temperature diffraction loop. Measurements were made on a Rigaku AFC8-Saturn 70 single-crystal X-ray diffractometer equipped with an X-stream 2000 low temperature system and a SHINE optic. Data were collected with Mo-K_α radiation. Data were collected and processed with the CrystalClear software (Rigaku).[61a,61b] Numerical absorption corrections were applied and the data were corrected for Lorentz and polarization effects. The structures were solved by direct methods (**L1H**, **1**, **3**, **4**, **5**, **6**, **7**),[61c] (**2**)[61d] and refined by Fourier techniques.[61e] Neutral atom scattering factors were taken from those provided by Cromer and Waber.[61f] Anomalous dispersion effects were included in F_{calc};[61g] the values for $\Delta f'$ and $\Delta f''$ were those of Creagh and McAuley.[61h] The values for the mass attenuation coefficients were those of Creagh and Hubbell.[61i] All calculations were performed with the CrystalStructure[61j,61k] crystallographic software package except for refinement, which was performed with SHELXL-97.[61c] Hydrogen atoms were introduced at calculated positions and refined with a riding model, unless otherwise indicated. All non-hydrogen atoms were refined anisotropically. For **L2H**, **1**, **3**, **5** and **6**, data collections, structural solutions, and refinements proceeded normally. For **L2H**, atom H1 was introduced into the refinement model according to its position in the difference map,and initially the atomic *x*, *y*, *z* coordinated were refined, but finally the atom was refined with a riding model. Friedel mates were averaged and the absolute configuration was not determined. The asymmetric unit of **1** contained a half-occupancy toluene molecule that was disordered over two sites. The toluene protons could not be located

Table 5. Summary of crystal data for compounds **L2**H, **1**–**5**.

	L2H	**1**	**2**	**3**	**5**
Formula	$C_{20}H_{34}N_2O$	$C_{47}H_{74}N_4O_2Zn$	$C_{38}H_{64}N_4O_2Zn_2$	$C_{58}H_{92}N_4O_2Zn_2$	$C_{79}H_{112}N_4O_4Zn_2$
Formula weight	318.50	792.51	739.71	1008.15	1312.54
Crystal system	triclinic	monoclinic	triclinic	triclinic	monoclinic
Space group	$P\bar{1}$	$C2/c$	$P\bar{1}$	$P\bar{1}$	$P2/c$
a [Å]	6.1799(14)	10.0658(11)	9.6308(9)	9.206(14)	24.314(4)
b [Å]	8.4415(18)	17.945(2)	11.0488(11)	11.540(19)	10.9529(17)
c [Å]	10.081(2)	25.003(3)	19.6721(19)	13.902(20)	28.023(4)
α [°]	67.242(7)	90	100.023(5)	92.493(13)	90
β [°]	78.354(11)	99.377(3)	97.146(5)	93.888(18)	94.232(4)
γ [°]	89.180(12)	90	108.791(4)	111.02(3)	90
V [Å^3]	473.76(17)	4455.8(9)	1914.6(3)	1372(4)	7442.7(20)
T [K]	153	153	153	153	153
Z	1	4	2	1	4
D_c [g/cm^3]	1.116	1.181	1.283	1.220	1.171
$F(000)$	176	1720	792	544	2824
μ(Mo-K_α)	0.68	5.92	12.89	9.18	6.94
Total reflections	3883	28248	20078	14165	96494
Unique reflections	1914	4605	20078	5600	15414
R_{int}	0.0167	0.0216	0.000	0.0314	0.0563
Observations	1904	4605	20078	5600	15414
Reflections $I > 2\sigma I$	209	4503	18150	5239	14312
R ($I > 2\sigma I$)	0.0348	0.0338	0.0905	0.0540	0.0643
w$R2$ (all reflections)	0.0961	0.0924	0.2538	0.1280	0.1574
GOF	1.049	1.038	1.144	1.120	1.172

from difference maps, and were omitted from the model. For **5**, one disordered amyl group was present (PART 1: [C32–35, C39] at 0.65 occupancy; PART 2: [C32A, C36–38, C40] at 0.35 occupancy). Hydrogen atoms on C33 and C36 were omitted from the model.

Complexes **2** and **7** were refined as non-merohedral twins with component #1 comprising 47.99% and 64.81% of the crystal, respectively (Tables 5 and 6). For **2**, a large negative residual density peak was present in the difference map (1.82 Å from H5A) and is likely a result of twinning that was not accounted for; overlap from the second twin domain caused errors in the intensities of some reflections. Complex **4** was refined as a merohedral twin, with component #1 comprising 19.60% of the crystal. The merohedral twin law was identified by the TwinRotMat function in the PLATON software.[611]

Table 6. Summary of crystal data for compounds **6**–**7**.

Compounds	**6**	**7**
Formula	$C_{44}H_{76}N_4O_4Zn_2$	$C_{56}H_{86}N_2O_4Zn_2$
Formula weight	855.87	982.07
Crystal system	triclinic	triclinic
Space group	$P\bar{1}$	$P\bar{1}$
a [Å]	8.960(3)	10.9384(15)
b [Å]	9.099(3)	11.4289(15)
c [Å]	14.779(6)	11.9898(16)
α [°]	81.33(3)	102.923(8)
β [°]	76.04(2)	106.541(7)
γ [°]	76.04(2)	107.637(8)
V [Å^3]	1123.8(7)	1288.1(3)
T [K]	153	153
Z	1	1
D_c [g/cm^3]	1.265	1.266
F(000)	460	528
μ(Mo-K_α)	11.11	9.77
Total reflections	8979	15846
Unique reflections	4141	15846
R_{int}	0.0939	0.000
Reflections $I > 2\sigma(I)$	2984	14915
Parameters	245	290
R [$I > 2\sigma(I)$]	0.1060	0.1061
wR2 (all reflections)	0.2132	0.2854
GOF	1.149	1.248

CCDC-762217 (for **L2H**), -762221 (for **1**), -762220 (for **2**), -762222 (for **3**), -833271 (for **4**), -762223 (for **5**), -833272 (for **6**), -833273 (for **7**) contain the supplementary crystallographic data for this paper. These data can be obtained free of charge from The Cambridge Crystallographic Data Centre via www.ccdc.cam.ac.uk/data_request/cif.

Synthetic Procedures

L1H: Water (80 mL), 2-*tert*-butyl-4-methylphenol (10.10 g, 61.5 mmol) and formaldehyde 37% solution in water (5 mL, 61.5 mmol) were added to 250 mL round-bottom flask equipped with a stir bar and a condenser. 1-Methylpiperazine (6.8 mL, 61.5 mmol) was added dropwise to the stirred solution. The resulting mixture was heated at reflux for 18 h. Upon cooling to room temperature a two phase mixture was formed. The organic layer (solid) was isolated, washed with methanol and dried under vacuum to remove any unreacted organic components. The resulting pale grey solid was recrystallized from methanol to give colourless crystals; yield 16.71 g, 98%. m.p. 90 °C. MS (AP-CI, MeOH): m/z = 277 (M^+, 100%). $C_{17}H_{28}N_2O$ (276.42): calcd. C 73.87, H 10.21, N 10.13; found C 73.81, H 10.10, N 10.66. ^{1}H NMR ($CDCl_3$, 500 MHz, 298 K): δ = 10.90 (s, 1 H, ArO*H*), 6.99 (s, 1 H, Ar*H*), 6.67 (s, 1 H, Ar*H*), 3.65 (s, 2 H, Ar–C*H*$_2$–N), 2.51 (br, 8 H, NC*H*$_2$C*H*$_2$N), 2.31 (s, 3 H, NC*H*$_3$), 2.23 (s, 3 H, ArCC*H*$_3$) 1.40 [s, 9 H, ArC–C(C*H*$_3$)$_3$] ppm. ^{13}C{^{1}H} NMR ($CDCl_3$, 125 MHz, 298 K): δ = 154.7 (Ar*C*–OH), 136.6 (Ar*C*–CH$_2$–N), 127.7 (Ar*C*H), 127.5 (Ar*C*H), 127.0 [Ar*C*–C(CH$_3$)$_3$], 121.6 (Ar*C*CH$_3$), 62.1 (ArC–*C*H$_2$–N), 55.3 (N–*C*H$_2$–CH$_2$–N), 52.7 (N–CH$_2$–*C*H$_2$–N), 46.3 (*C*H$_3$–N), 35.0 [ArC–*C*(CH$_3$)$_3$], 30.0 [ArC–C–(*C*H$_3$)]$_3$, 21.2 (ArC–*C*H$_3$) ppm.

L2H: This compound was prepared in the same manner as described above for **L1**H with 2,6-di-*tert*-butylphenol (12.69 g, 61.5 mmol), formaldehyde 37% solution in water (5 mL, 61.5 mmol), and 1-methyl piperazine (6.8 mL, 61.5 mmol) as starting materials. The product was recrystallized to yield a colourless crystalline solid; yield 17.65 g, 90%. m.p. 119 °C. MS (MALDI, anthracene matrix): m/z = 381 (M^+, 100%). $C_{20}H_{34}N_2O$ (318.50): calcd. C 75.42, H 10.76, N 8.80; found C 75.40, H 10.65, N 8.79. ^{1}H NMR ($CDCl_3$, 500 MHz, 298 K): δ = 11.49 (s, 1 H, ArO*H*), 7.26 (s, 1 H, Ar*H*), 6.93 (s, 1 H, Ar*H*), 3.75 (s, 2 H, Ar–C*H*$_2$–N), 2.98 (d, J = 10.2 Hz, 4 H, NC*H*$_2$CH$_2$N), 2.86 (d, J = 10.3 Hz, 4 H, NCH$_2$C*H*$_2$N), 2.35 (s, 3 H, NC*H*$_3$), 1.42 [s, 9 H, C(C*H*$_3$)$_3$], 1.29 [s, 9 H, C(C*H*$_3$)$_3$] ppm. ^{13}C{^{1}H} NMR ($CDCl_3$, 125 MHz, 298 K): δ = 154.5 (Ar*C*OH), 140.9 [Ar*C*C(CH$_3$)$_3$], 135.8 [Ar*C*–C(CH$_3$)$_3$], 123.8 (Ar*C*H), 123.3 (Ar*C*H), 120.9 (Ar*C*–CH$_2$), 62.5 (*C*H$_3$–N), 55.3 (N–*C*H$_2$–CH$_2$–N), 52.7 (N–CH$_2$–*C*H$_2$–N), 46.3 (ArC–*C*–CH$_2$), 35.2 [ArC–*C*(CH$_3$)$_3$], 34.5 [ArC–*C*(CH$_3$)$_3$], 32.1 [ArC–C–(*C*H$_3$)]$_3$, 30.0 [ArC–C–(*C*H$_3$)]$_3$ ppm.

L3H: Water (100 mL), 2,6-di-*tert*-amylphenol (18.99 g, 81.0 mmol) and formaldehyde 37% solution in water (6.6 mL, 81.0 mmol) were added to a 500 mL round-bottom flask equipped with a stir bar and a condenser. 1-Methyl piperazine (8.1 g, 81.0 mmol) was added dropwise to the stirred solution. The resulting mixture was heated at reflux for 18 h. Upon cooling to room temperature a two phase mixture formed. The organic material was extracted with diethyl ether and dried with magnesium sulfate. The solvent was removed by rotary evaporation to give a pale brown oil from which colourless crystals were obtained upon standing for several days under ambient conditions; yield 23.02 g, 82%. m.p. 82 °C. MS (AP-CI, MeOH): m/z = 347 (M^+, 100%). $C_{22}H_{38}NO_2$ (348.55): calcd. C 76.25, H 11.05, N 8.08; found C 76.36, H 10.80, N 8.04. ^{1}H NMR ($CDCl_3$, 500 MHz, 298 K): δ = 10.77 (s, 1 H, ArO*H*), 7.07 (d, J = 2.2 Hz, 1 H, Ar*H*), 6.75 (d, J = 2.2 Hz, 1 H, Ar*H*), 3.67 (s, 2 H, ArC–C*H*$_2$–N), 2.53 (br, 8 H, N–C$_2$*H*$_4$–N), 2.30 (s, 3 H, NC*H*$_3$), 1.88 (q, J = 7.4 Hz, 2 H, CC*H*$_2$CH$_3$), 1.56 (q, J = 7.4 Hz, 2 H, CC*H*$_2$CH$_3$), 1.36 [s, 6 H, ArC–C(C*H*$_3$)$_2$], 1.23 [s, 6 H, ArC–C(C*H*$_3$)$_2$], 0.65 (t, J = 7.4 Hz, 3 H, CH$_2$C*H*$_3$), 0.64 (t, J = 7.4 Hz, 3 H, CH$_2$C*H*$_3$) ppm. ^{13}C{^{1}H} NMR ($CDCl_3$, 500 MHz, 298 K): δ = 154.2 (Ar*C*–OH), 139.0 [Ar*C*C(CH$_3$)$_3$], 134.1 [Ar*C*–C(CH$_3$)$_3$], 125.3 (Ar*C*H), 124.4 (Ar*C*H), 120.6 (Ar*C*–CH$_2$–N), 62.5 (N–*C*H$_2$–C), 55.3 (N–*C*H$_2$–CH$_2$–N), 52.3 (N–CH$_2$–*C*H$_2$–N), 46.3 {ArC–*C*[(CH$_3$)$_2$–CH$_2$]}, 38.7 (N–*C*H$_3$), 37.6 {C[(CH$_3$)$_2$–*C*H$_2$]}, 37.5 {C–[(CH$_3$)$_2$–*C*H$_2$]}, 33.4 {ArC–*C*[(CH$_3$)$_2$–CH$_2$]}, 28.9 {C[(*C*H$_3$)$_2$–CH$_2$]}, 28.0 {C[(*C*H$_3$)$_2$–CH$_2$]}, 9.8 (CH$_2$–*C*H$_3$), 9.5 (CH$_2$–*C*H$_3$) ppm.

L4H: Water (80 mL), 2-*tert*-butyl-4-methylphenol (16.51 g, 80.0 mmol) and formaldehyde 37% solution in water (6.50 mL, 80.0 mmol) were added to 250 mL round-bottom flask equipped with a stir bar and a condenser. Morpholine (6.97 mL, 80.0 mmol) was added dropwise to the stirred solution. The resulting mixture was heated at reflux for 18 h. Upon cooling to room temperature a two phase mixture was formed. The organic layer (solid) was isolated, washed with methanol and dried under vacuum to remove any unreacted organic components. The resulting brown gel-like solid was recrystallized from methanol to give a colourless solid;

yield 21.23 g, 87%. m.p. 112 °C. MS (MALDI, anthracene matrix): *m*/*z* = 305 (M^+, 100%). $C_{19}H_{31}NO_2$ (305.46): calcd. C 74.71, H 10.23, N 4.59; found C 74.66, H 10.27, N 4.52. ^{1}H NMR ($CDCl_3$, 500 MHz, 298 K): δ = 10.66 (s, 1 H, ArO*H*), 7.23 (d, *J* = 2.2 Hz, 1 H, Ar*H*), 6.84 (d, *J* = 2.2 Hz, 1 H, Ar*H*), 3.75 (s, 2 H, Ar–CH_2–N), 3.68 (br, 4 H, $OC_2H_4C_2H_4N$) 2.56 (br, 4 H, $OC_2H_4C_2H_4N$), 1.41 [s, 9 H, C(CH_3)$_3$], 1.28 [s, 9 H, C(CH_3)$_3$] ppm. ^{13}C{^{1}H} NMR ($CDCl_3$, 125 MHz, 298 K): δ = 154.4 (Ar*C*–OH), 141.2 [Ar*C*–C(CH$_3$)$_3$], 136.0 [Ar*C*–C(CH$_3$)$_3$], 124.0 (Ar*C*H), 123.6 (Ar*C*H), 120.5 (Ar*C*–CH$_2$), 67.2 (O–*C*$_2$H$_4$–C$_2$H$_4$-N), 63.1 (ArC*C*H$_2$N), 53.2 (O–C$_2$H$_4$–*C*$_2$H$_4$–N), 35.3 [ArC–*C*(CH$_3$)$_3$], 34.6 [ArC–*C*(CH$_3$)$_3$], 32.1 [ArC–C–(*C*H$_3$)]$_3$, 30.0 [ArC–C–(*C*H$_3$)]$_3$ ppm.

Zn[ONN^{tBu,tBu}]$_2$ (1): This compound was prepared in the same manner as described below for **2** with diethylzinc (1.7 mL, 2.0 mmol, 15 wt.-% in hexane) and **L2**H (0.64 g, 2.0 mmol) as starting materials. **1** was obtained as a colourless crystalline solid; yield 1.07 g, 77%. Crystals suitable for X-ray crystallography could be grown by slow evaporation, or by cooling at –35 °C, of a saturated toluene/hexane solution. $C_{47}H_{74}N_4O_2Zn(C_7H_8)$ (792.5 + 92.1 = 884.6): calcd. C 71.23, H 9.41, N 7.07; found C 71.10, H 9.49, N 7.05. ^{1}H NMR (C_5D_5N, 500 MHz, 343 K): δ = 7.58 (s, 1 H, Ar*H*), 7.11 (s, 1 H, Ar*H*), 4.07 (s, 2 H, Ar–CH_2–N), 3.07 (br, 4 H, NCH_2CH$_2$N), 2.83 (s, 4 H, NCH$_2$CH_2N), 2.29 (s, 3 H, NCH_3), 1.60 [s, 9 H, C(CH_3)$_3$], 1.44 [s, 9 H, C(CH_3)$_3$] ppm. ^{13}C{^{1}H} NMR (C_5D_5N, 125 MHz, 298 K): δ = 165.3 (Ar*C*–O), 137.8 (Ar*C*–CH$_2$N), 134.5 [Ar*C*–C(CH$_3$)$_3$], 129.6 (*C*H), 128.9 (*C*H), 122.1 [Ar*C*–C(CH$_3$)$_3$], 64.6 (ArC*C*H$_2$N), 55.1 (N–*C*H$_2$–CH$_2$–N), 53.5 (N–CH$_2$–*C*H$_2$–N), 46.1 (*C*H$_3$–N), 36.0 [ArC–*C*(CH$_3$)$_3$], 34.4 [ArC–*C*(CH$_3$)$_3$], 32.6 [C(*C*H$_3$)$_3$], 30.5 [C(*C*H$_3$)$_3$] ppm.

{[μ-ONN^{Me,tBu}]ZnEt}$_2$ (2): To a 50 mL flask containing diethylzinc (6.2 mL, 5.02 mmol, 15 wt.-% in hexane) a solution of **L1**H (1.39 g, 5.02 mmol) in toluene (2.0 mL) that was cooled to –35 °C was added dropwise. The colourless mixture was warmed, while being stirred, to room temperature and then held at this temperature for 18 h. Volatiles were removed under vacuum to give a white residue, which was washed with hexane (2 × 4 mL) and dried in vacuo. The crude product was recrystallized from a saturated toluene solution held at –35 °C to give **2** as a colourless crystalline solid; yield 1.43 g, 77%. $C_{38}H_{64}N_4O_2Zn_2$ (739.71): calcd. C 61.70, H 8.72, N 7.57; found C 62.02, H 9.13, N 7.98. ^{1}H NMR (C_5D_5N, 500 MHz, 343 K): δ = 7.33 (s, 1 H, Ar*H*), 6.84 (s, 1 H, Ar*H*), 4.00 (s, 2 H, Ar–CH_2–N), 3.04 (br, 4 H, N CH_2CH_2N), 2.83 (br, 4 H, NCH_2CH_2N), 2.35 (s, 3 H, NCH_3), 2.30 (s, 3 H, ArC–CH_3), 1.78 (s, 2 H, CH_2CH$_3$), 1.58 [q, 9 H, ArC–C(CH_3)$_3$], 0.91 (t, 3 H, CH$_2$CH_3) ppm. ^{13}C{^{1}H} NMR (C_5D_5N, 125 MHz, 298 K): δ = 164.4 (Ar*C*–O), 138.6 (*C*–CH$_2$N), 130.4 (Ar*C*H), 128.7 (Ar*C*H), 121.9 [*C*–C(CH$_3$)$_3$], 120.8 [*C*(CH$_3$)], 64.6 (N–*C*H$_2$–C), 55.4 (N–*C*H$_2$–CH$_2$–N), 53.0 (N–CH$_2$–*C*H$_2$–N), 45.9 (Ar–*C*H$_2$–N), 35.5 (*C*H$_3$–N), 30.6 [C(*C*H$_3$)$_3$], 30.4 [*C*(CH$_3$)$_3$], 21.4 (CH$_3$*C*H$_2$), 21.2 [C(*C*H$_3$)], 14.1 (*C*H$_3$CH$_2$) ppm.

{[μ-ONN^{tBu,tBu}]ZnEt}$_2$ (3): To a 50 mL flask containing diethylzinc (3.3 mL, 4.0 mmol, 15 wt.-% in hexane) a solution of **L2**H (0.64 g, 2.0 mmol) in toluene (2.0 mL) that was cooled to –35 °C was added dropwise. The colourless mixture was warmed, while being stirred, to room temperature and then held at this temperature for 18 h. Volatiles were removed under vacuum to give a white residue, which was washed with hexane (2 × 4 mL) and dried in vacuo; yield 0.92 g, 56%. Crystals suitable for X-ray crystallography could be grown by slow evaporation, or by cooling at –35 °C, of a saturated toluene/hexane solution. $C_{44}H_{76}N_4O_2Zn_2$ (823.87): calcd. C 64.14, H 9.30, N 6.80; found C 63.72, H 9.21, N 6.10. ^{1}H NMR (C_5D_5N, 500 MHz, 358 K): δ = 7.63 (s, 1 H, Ar*H*), 7.10 (s, 1 H, Ar*H*), 3.65 (s, 2 H, Ar–CH_2–N), 2.64 (br, 4 H, NCH_2CH$_2$N), 2.54 (s, 4 H, NCH$_2$CH_2N), 2.27 (s, 3 H, NCH_3), 1.81 [s, 9 H, C(CH_3)$_3$], 1.57 (t, *J* = 8.0 Hz, 3 H, CH_3CH$_2$), 1.50 [s, 9 H, C(CH_3)$_3$], 0.59 (q, *J* = 8.0 Hz, 2 H, CH$_3$CH_2) ppm. ^{13}C{^{1}H} NMR (C_5D_5N, 125 MHz, 298 K): δ = 165.3 (Ar*C*–O), 138.3 (Ar*C*–CH$_2$N), 134.5 [Ar*C*–C(CH$_3$)$_3$], 126.6 (Ar*C*H), 126.0 (Ar*C*H), 122.1 [Ar*C*–C(CH$_3$)$_3$], 64.6 (ArC–*C*H$_2$–N), 55.2 (N–*C*H$_2$–CH$_2$–N), 53.5 (N–CH$_2$–*C*H$_2$–N), 46.1 (*C*H$_3$–N), 36.0 [*C*(CH$_3$)$_3$], 34.4 [*C*(CH$_3$)$_3$], 32.6 [C(*C*H$_3$)$_3$], 30.5 [C(*C*H$_3$)$_3$], 14.1 (*C*H$_3$CH$_2$), 1.5 (CH$_3$*C*H$_2$) ppm.

{[μ-ONN^{tAm,tAm}]ZnEt}$_2$ (4): To a 50 mL flask containing diethylzinc (6.2 mL, 5.02 mmol, 10 wt.-% in hexane) a solution of **L3**H (1.74 g, 5.02 mmol) in toluene (2.0 mL) that was cooled to –35 °C was added dropwise. The colourless mixture was warmed, while being stirred, to room temperature and then held at this temperature for 18 h. Volatiles were removed under vacuum to give a white residue, which was washed with hexane (2 × 4 mL) and dried in vacuo. The crude product was recrystallized from a saturated toluene solution at –35 °C to give **4** as a colourless crystalline solid; yield 1.92 g, 87%. $C_{48}H_{84}N_4O_2Zn_2$ (879.98): calcd. C 65.51, H 9.62, N 6.37; found C 65.47, H 10.89, N 6.28. ^{1}H NMR (C_5D_5N, 500 MHz, 358 K): δ = 7.49 (s, 1 H, Ar*H*), 7.04 (s, 1 H, Ar*H*), 3.65 (s, 2 H, ArC–CH_2–N), 2.64 (br, 4 H, NCH_2CH$_2$N), 2.56 (s, 4 H, NCH$_2$CH_2N), 2.41 (q, *J* = 7.4 Hz, 2 H, CCH_2CH$_3$), 2.27 (s, 3 H, NCH_3), 1.80 (q, *J* = 7.4 Hz, 2 H, CCH_2CH$_3$), 1.74 [s, 6 H, C(CH_3)$_2$], 1.59 (t, *J* = 8.0 Hz, 3 H, CH_3CH$_2$), 1.46 [s, 6 H, C(CH_3)$_2$], 0.98 (t, *J* = 7.4 Hz, 3 H, CH$_2$CH_3), 0.91 (t, *J* = 7.4 Hz, 3 H, CH$_2$CH_3), 0.61 (q, *J* = 8.0 Hz, 2 H, CH$_3$CH_2) ppm. ^{13}C{^{1}H} NMR (C_5D_5N, 125 MHz, 298 K): δ = 165.2 (Ar*C*–O), 132.4 (Ar*C*–CH$_2$–N), 127.3 (Ar*C*H), 126.4 (Ar*C*H), 121.8 {Ar*C*–C[(CH$_3$)$_2$–CH$_2$]}, 64.5 (ArC–*C*H$_2$–N), 55.1 (N–*C*H$_2$–CH$_2$–N), 53.5 (N–CH$_2$–*C*H$_2$–N), 46.1 (N–*C*H$_3$), 39.42 {C[(CH$_3$)$_2$–*C*H$_2$]}, 37.9 {*C*[(CH$_3$)$_2$–CH$_2$]}, 37.5 {C[(CH$_3$)$_2$–*C*H$_2$]}, 33.3 {*C*[(CH$_3$)$_2$–CH$_2$]}, 29.6–28.5 {C[(CH$_3$)$_2$–*C*H$_2$]}, 14.1 (*C*H$_3$CH$_2$) 10.7–9.9 [(CH$_3$)$_2$–CH$_2$–*C*H$_3$], 1.6 (CH$_3$*C*H$_2$) ppm.

{[ONN^{tAm,tAm}]Zn(μ-OBn)}$_2$ (5): To a solution of **4** (0.80 g, 0.91 mmol) in toluene (5 mL) that was cooled to –35 °C BnOH (190 μL, 1.8 mmol) was added dropwise. The reaction mixture was warmed, while being stirred, to room temperature and then held at this temperature for 3 h. The solvent was removed under vacuum to give a white residue, which was washed with cold hexane (2 × 4 mL) and dried in vacuo. The crude product was recrystallized from toluene/hexane to give **5** as a colourless crystalline solid; yield 0.84 g, 89%. $C_{58}H_{88}N_4O_4Zn_2$ (1036.12): calcd. C 67.23, H 8.56, N 5.41; found C 67.78, H 9.12, N 5.63. ^{1}H NMR (C_5D_5N, 500 MHz, 343 K): δ = 7.69 (s, 1 H, Ar*H*), 7.51 (s, 2 H, Ar*H*), 7.43 (s, 1 H, Ar*H*), 7.37 (s, 1 H, Ar*H*), 7.05 (s, 2 H, Ar*H*), 5.11 (br, 2 H, OCH_2Ar), 4.09 (s, 2 H, ArC–CH_2–N), 2.60–3.05 (br, 8 H, overlapping, N–C$_2$H$_4$–N), 1.77 (m, 4 H, CCH_2CH$_3$), 1.58 (s, 3 H, NCH_3), 1.41 [s, 6 H, C(CH_3)$_2$], 1.38 [s, 6 H, C(CH_3)$_2$], 0.87 (m, 6 H, CH$_2$CH_3) ppm. ^{13}C{^{1}H} NMR (C_5D_5N, 125 MHz, 298 K): δ = 163.8 (Ar*C*–O), 144.5 (Ar*C*–CH$_2$), 133.6 (Ar*C*–CH$_2$–N), 129.1 (Ar*C*), 129.0 (Ar*C*), 128.0 (Ar*C*H), 127.3 (Ar*C*H), 126.8 (Ar*C*), 119.9 {Ar*C*–C[(CH$_3$)$_2$–CH$_2$]}, 69.4 (ArC–*C*H$_2$), 65.0 (ArC–*C*H$_2$–N), 55.3 (N–*C*H$_2$–CH$_2$–N), 54.2 (N–CH$_2$–*C*H$_2$–N), 45.9 (N–*C*H$_3$), 39.1 {C[(CH$_3$)$_2$–*C*H$_2$]}, 37.8 {*C*[(CH$_3$)$_2$–CH$_2$]}, 37.5 {C[(CH$_3$)$_2$–*C*H$_2$]}, 33.4 {*C*[(CH$_3$)$_2$–CH$_2$]}, 29.4–28.5 {C[(CH$_3$)$_2$–*C*H$_2$]}, 10.4–9.9 [(CH$_3$)$_2$–CH$_2$–*C*H$_3$] ppm.

{[ONN^{tBu,tBu}]Zn(μ-OEt)}$_2$ (6): To a 50 mL flask containing diethylzinc (7.8 mL, 6.3 mmol, 15 wt.-% in hexane) a solution of **L2**H (2.00 g, 6.3 mmol) in toluene (2.0 mL) cooled to –35 °C was added dropwise. The colourless mixture was warmed, while being stirred, to room temperature and then held at this temperature for 3 h.

Volatiles were removed under vacuum to give an off-white residue, which was washed with pentane (2 × 4 mL) and redissolved in toluene (2.0 mL). To this solution EtOH (366 μL, 6.3 mmol) was added dropwise, and the reaction mixture was stirred at room temperature for 18 h. The resulting mixture was filtered and the filtrate was concentrated under vacuum and cooled to –35 °C to afford **6** as a colourless crystalline solid; yield 1.65 g, 61%. $C_{44}H_{76}N_4O_4Zn_2$ (855.87): calcd. C 61.75, H 8.95, N 6.55; found C 61.69, H 9.19, N 7.00. ^{1}H NMR (C_5D_5N, 500 MHz, 358 K): δ = 7.72 (s, 1 H, Ar*H*), 7.66 (s, 1 H, Ar*H*), 4.04 (br, 2 H, OCH_2CH_3), 3.83 (s, 2 H, Ar–CH_2–N), 3.00 (br, 4 H, NCH_2CH_2N), 2.79 (br, 4 H, NCH_2CH_2N), 2.53 (s, 3 H, NCH_3), 1.92 [s, 9 H, $C(CH_3)_3$], 1.58 [s, 9 H, $C(CH_3)_3$], 1.55 (t, 3 H, OCH_2CH_3) ppm. ^{13}C{^{1}H} NMR (C_5D_5N, 125 MHz, 298 K): δ = 164.2 (Ar*C*–O), 138.1 (*C*–CH_2N), 126.4 (Ar*C*H), 126.1 (Ar*C*H), 119.9 [*C*–$C(CH_3)_3$], 119.7 [*C*–$C(CH_3)_3$], 65.6 (N–*C*H_2–C), 55.3 (N–*C*H_2–CH_2–N), 54.1 (N–CH_2–*C*H_2–N), 46.1 (*C*H_3–N), 45.8 (OCH_2CH_3) 36.0 [*C*$(CH_3)_3$], 35.6 [*C*$(CH_3)_3$], 34.3 (OCH_2CH_3) 32.4 [C(*C*$H_3)_3$], 30.5 [C(*C*$H_3)_3$] ppm.

{[μ-ONO^{rBu,rBu}]ZnEt}$_2$ (7): To a 50 mL flask containing diethylzinc (6.2 mL, 5.02 mmol, 15 wt.-% in hexane) a solution of **L4**H (1.53 g, 5.02 mmol) in toluene (2.0 mL) cooled at –35 °C was added dropwise. The colourless mixture was warmed, while being stirred, to room temperature and then held at this temperature for 18 h. Volatiles were removed under vacuum to give a white residue, which was washed with hexane (2 × 4 mL) and dried in vacuo; yield 1.62 g, 81%. Crystals suitable for X-ray crystallography could be grown by slow evaporation, or by cooling at –35 °C, of a saturated toluene solution. $C_{42}H_{70}N_4O_4Zn_2$ (825.80): calcd. C 63.23, H 8.84, N 3.51; found C 63.16, H 8.55, N 3.60. ^{1}H NMR (C_5D_5N, 500 MHz, 313 K): δ = 7.63 (s, 1 H, Ar*H*), 7.10 (s, 1 H, Ar*H*), 3.81 (br, 4 H, $OC_2H_4C_2H_4N$), 3.59 (s, 2 H, Ar–CH_2–N), 2.50 (br, 4 H, $OC_2H_4C_2H_4N$), 1.79 [s, 9 H, $C(CH_3)_3$], 1.59 (t, *J* = 8.0 Hz, 3 H, CH_3CH_2), 1.48 [s, 9 H, $C(CH_3)_3$], 0.58 (q, *J* = 8.0 Hz, 2 H, CH_3CH_2) ppm. ^{13}C{^{1}H} NMR (C_5D_5N, 125 MHz, 298 K): δ = 165.35 (Ar*C*–O), 141.2 [Ar*C*–$C(CH_3)_3$], 137.93 (Ar*C*–CH_2N), 134.70 [Ar*C*–$C(CH_3)_3$], 126.73 (Ar*C*H), 124.44 (Ar*C*H), 121.57 [Ar*C*–$C(CH_3)_3$], 65.55 (O–C_2H_4–C_2H_4–N), 65.45 (O–C_2H_4–C_2H_4–N), 65.13 (ArCCH_2N), 36.01 [ArC–*C*$(CH_3)_3$], 34.41 [ArC–*C*$(CH_3)_3$], 32.60 [ArC–C–(*C*H_3)]$_3$, 30.48 [ArC–C–(*C*H_3)]$_3$, 13.98 (CH_3CH_2), 0.76 (CH_3CH_2) ppm.

Typical Solution Polymerization Procedure: The reaction mixtures were prepared in a glovebox and subsequent operations were performed with standard Schlenk techniques. A monomer:initiator ratio of 100:1 was employed. A sealable Schlenk tube containing a stir bar and the monomer (0.05 mmol) in toluene (8.00 mL) was heated to the desired temperature, then the initiator solution (26.3 mM), which was taken from a stock solution containing a prescribed amount of ROH, was added to the tube. The mixture was stirred for the allotted time. An aliquot of the reaction solution was taken for NMR spectroscopic analysis, and the reaction was quenched immediately by the addition of methanol. The resulting solid was dissolved in dichloromethane and the polymer precipitated with excess cold methanol. The polymer was collected by filtration, washed with methanol to remove any unreacted monomer, and dried under reduced pressure.

Bulk Polymerization Procedure: For solvent free polymerizations of LA, the monomer:initiator ratio employed was 100:1 and the reactions were conducted at 130 °C. A Schlenk tube equipped with magnetic stir bar was charged in a glovebox with the required amount of LA (0.50 g, 3.5 mmol) and initiator (0.042–0.015 g). The reaction vessel was sealed, brought out of the glovebox and immersed in an oil bath that was preheated to 130 °C. At the desired time an aliquot (ca 0.3 mL) was withdrawn from the flask for ^{1}H NMR analysis to determine the monomer conversion. The reaction was quenched with methanol and the resulting solid was dissolved in dichloromethane, precipitated with excess cold methanol, then filtered and dried under reduced pressure.

Typical Microwave-Assisted Ring-Opening Polymerization: To a microwave vial charged with LA (576 mg, 5.27 mmol) or ε-CL (601 mg, 5.27 mmol) in toluene (10 mL), a toluene solution (2.00 mL) of the initiator containing a prescribed amount of benzyl or *tert*-butyl alcohol was added. The vial was sealed with a septum and the mixture was irradiated to a constant required temperature for the desired amount of time. After irradiation, the vial was cooled to room temperature, an aliquot of the product was taken for NMR spectroscopic analysis, and the reaction was quenched immediately by the addition of methanol. The resulting solid was dissolved in dichloromethane and the polymer precipitated with excess cold methanol. A colourless product was collected by filtration, washed with methanol to remove any unreacted monomer, and dried under reduced pressure.

CO_2-Cyclohexene Oxide Reactions: The complex (0.2 mol-%) was dissolved in cyclohexene oxide (2.27 g, 23.2 mmol) that was held in a glovebox. The mixture and cocatalyst (0.2 mol-%) was placed in a predried autoclave equipped with a pressure gauge. The autoclave was sealed, removed from the glovebox and attached to an overhead magnetic stirrer. The system was pressurized to approx. 40 bar with CO_2 and heated (as with all processes under high pressure, appropriate safety precautions must be taken). The mixture was stirred for the desired amount of time and then the pressure was slowly released whilst the pressure vessel was cooled in an ice-bath. A small amount of the residue in the vessel was removed for ^{1}H NMR analysis.

Supporting Information (see footnote on the first page of this article): ^{1}H NMR and MALDI-TOF MS spectra of **L2**H, representative homodecoupled ^{1}H NMR spectra of PLA, diagrams of the molecular structures of **4** and **5**, and $\ln([LA]_0/[LA]_t)$ vs. time plot for the bulk polymerization of LA.

Acknowledgments

We thank Natural Sciences and Engineering Research Council of Canada (NSERC) of Canada, the Canada Foundation for Innovation, the Provincial Government of Newfoundland and Labrador, and Memorial University for financial support. J. M. B. S. thanks Women in Science and Engineering High-School Summer Student Employment Program. N. I. thanks Dr. Pawel Horeglad (University of Warsaw) for advice on tacticity calculations.

[1] D. J. Doyle, V. C. Gibson, A. J. P. White, *Dalton Trans.* **2007**, 358.
[2] C.-A. Huang, C.-L. Ho, C.-T. Chen, *Dalton Trans.* **2008**, 3502.
[3] C.-A. Huang, C.-T. Chen, *Dalton Trans.* **2007**, 5561.
[4] J. Ejfler, K. Krauzy-Dziedzic, S. Szafert, L. B. Jerzykiewicz, P. Sobota, *Eur. J. Inorg. Chem.* **2010**, 3602.
[5] X. Zhang, T. J. Emge, K. C. Hultzsch, *Organometallics* **2010**, *29*, 5871.
[6] A. D. Schofield, M. L. Barros, M. G. Cushion, A. D. Schwarz, P. Mountford, *Dalton Trans.* **2009**, 85.
[7] W.-C. Hung, C.-C. Lin, *Inorg. Chem.* **2009**, *48*, 728.
[8] L. E. Breyfogle, C. K. Williams, J. V. G. Young, M. A. Hillmyer, W. B. Tolman, *Dalton Trans.* **2006**, 928.
[9] E. L. Marshall, V. C. Gibson, H. S. Rzepa, *J. Am. Chem. Soc.* **2005**, *127*, 6048.

[10] Y. Sarazin, V. Poirier, T. Roisnel, J.-F. Carpentier, *Eur. J. Inorg. Chem.* **2010**, 3423.
[11] D. J. Darensbourg, W. Choi, O. Karroonnirun, N. Bhuvanesh, *Macromolecules* **2008**, *41*, 3493.
[12] H. E. Dyer, S. Huijser, A. D. Schwarz, C. Wang, R. Duchateau, P. Mountford, *Dalton Trans.* **2008**, 32.
[13] A. Amgoune, C. M. Thomas, J.-F. Carpentier, *Macromol. Rapid Commun.* **2007**, *28*, 693.
[14] G. Labourdette, D. J. Lee, B. O. Patrick, M. B. Ezhova, P. Mehrkhodavandi, *Organometallics* **2009**, *28*, 1309.
[15] L. Wang, H. Ma, *Dalton Trans.* **2010**, *39*, 7897.
[16] C. K. Williams, L. E. Breyfogle, S. K. Choi, W. Nam, V. G. Young, M. A. Hillmyer, W. B. Tolman, *J. Am. Chem. Soc.* **2003**, *125*, 11350.
[17] M. H. Chisholm, J. C. Gallucci, H. Zhen, J. C. Huffman, *Inorg. Chem.* **2001**, *40*, 5051.
[18] M. H. Chisholm, Z. Zhou, *J. Mater. Chem.* **2004**, *14*, 3081.
[19] C. K. Williams, N. R. Brooks, M. A. Hillmyer, W. B. Tolman, *Chem. Commun.* **2002**, 2132.
[20] J. Lewiński, P. Horeglad, M. Dranka, I. Justyniak, *Inorg. Chem.* **2004**, *43*, 5789.
[21] S. Groysman, E. Sergeeva, I. Goldberg, M. Kol, *Inorg. Chem.* **2005**, *44*, 8188.
[22] S. Gendler, S. Segal, I. Goldberg, Z. Goldschmidt, M. Kol, *Inorg. Chem.* **2006**, *45*, 4783.
[23] L. M. Broomfield, Y. Sarazin, J. A. Wright, D. L. Hughes, W. Clegg, R. W. Harrington, M. Bochmann, *J. Organomet. Chem.* **2007**, *692*, 4603.
[24] J.-T. Issenhuth, J. Pluvinage, R. Welter, S. Bellemin-Laponnaz, S. Dagorne, *Eur. J. Inorg. Chem.* **2009**, 4701.
[25] V. Poirier, T. Roisnel, J.-F. Carpentier, Y. Sarazin, *Dalton Trans.* **2011**, *40*, 523.
[26] J. D. Farwell, P. B. Hitchcock, M. F. Lappert, G. A. Luinstra, A. V. Protchenko, X.-H. Wei, *J. Organomet. Chem.* **2008**, *693*, 1861.
[27] L. Nikolic, I. Ristic, B. Adnadjevic, V. Nikolic, J. Jovanovic, M. Stankovic, *Sensors* **2010**, *10*, 5063.
[28] S. Jing, W. Peng, Z. Tong, Z. Baoxiu, *J. Appl. Polym. Sci.* **2006**, *100*, 2244.
[29] M. R. Kember, A. Buchard, C. K. Williams, *Chem. Commun.* **2011**, *47*, 141.
[30] M. North, R. Pasquale, C. Young, *Green Chem.* **2010**, *12*, 1514.
[31] K. L. Collins, L. J. Corbett, S. M. Butt, G. Madhurambal, F. M. Kerton, *Green Chem. Lett. Rev.* **2007**, *1*, 31.
[32] F. M. Kerton, S. Holloway, A. Power, R. G. Soper, K. Sheridan, J. M. Lynam, A. C. Whitwood, C. E. Willans, *Can. J. Chem.* **2008**, *86*, 435.
[33] J. Ejfler, S. Szafert, K. Mierzwicki, L. B. Jerzykiewicz, P. Sobota, *Dalton Trans.* **2008**, 6556.
[34] A. Gao, Y. Mu, J. Zhang, W. Yao, *Eur. J. Inorg. Chem.* **2009**, 3613.
[35] K. Nakano, K. Nozaki, T. Hiyama, *J. Am. Chem. Soc.* **2003**, *125*, 5501.
[36] I. J. Bruno, J. C. Cole, M. Kessler, J. Luo, W. D. S. Momerwell, L. H. Purkis, B. R. Smith, R. Taylor, R. I. Cooper, S. E. Harris, A. G. Orpen, *J. Chem. Inf. Comput. Sci.* **2004**, *44*, 2133.
[37] J. Hunger, S. Blaurock, J. Sieler, *Z. Anorg. Allg. Chem.* **2005**, *631*, 472.
[38] M. R. P. Van Vliet, J. T. B. H. Jastrzebski, G. Van Koten, K. Vrieze, A. L. Spek, *J. Organomet. Chem.* **1983**, *251*, c17.
[39] H.-Y. Chen, H.-Y. Tang, C.-C. Lin, *Macromolecules* **2006**, *39*, 3745.
[40] A. Banerjee, S. Ganguly, T. Chattopadhyay, K. Sabnam Banu, A. Patra, S. Bhattacharya, E. Zangrando, D. Das, *Inorg. Chem.* **2009**, *48*, 8695.
[41] K. Nakano, T. Hiyama, K. Nozaki, *Chem. Commun.* **2005**, 1871.
[42] Y. Sarazin, J. A. Wright, D. A. J. Harding, E. Martin, T. J. Woodman, D. L. Hughes, M. Bochmann, *J. Organomet. Chem.* **2008**, *693*, 1494.
[43] A. R. F. Cox, V. C. Gibson, E. L. Marshall, A. J. P. White, D. Yeldon, *Dalton Trans.* **2006**, 5014.
[44] C. M. Silvernail, L. J. Yao, L. M. R. Hill, M. A. Hillmyer, W. B. Tolman, *Inorg. Chem.* **2007**, *46*, 6565.
[45] F. Qian, K. Liu, H. Ma, *Dalton Trans.* **2010**, *39*, 8071.
[46] L. F. Sanchez-Barba, C. Alonso-Moreno, A. Garces, M. Fajardo, J. Fernandez-Baeza, A. Otero, A. Lara-Sanchez, A. M. Rodriguez, I. Lopez-Solera, *Dalton Trans.* **2009**, 8054.
[47] A. Garcés, L. F. Sánchez-Barba, C. Alonso-Moreno, M. Fajardo, J. Fernández-Baeza, A. Otero, A. Lara-Sánchez, I. López-Solera, A. M. Rodríguez, *Inorg. Chem.* **2010**, *49*, 2859.
[48] C. Zhang, Z.-X. Wang, *Appl. Organomet. Chem.* **2009**, *23*, 9.
[49] H. Zhu, E. Y. X. Chen, *Organometallics* **2007**, *26*, 5395.
[50] F. Drouin, P. O. Oguadinma, T. J. J. Whitehorne, R. E. Prud′homme, F. Schaper, *Organometallics* **2010**, *29*, 2139.
[51] B. M. Chamberlain, M. Cheng, D. R. Moore, T. M. Ovitt, E. B. Lobkovsky, G. W. Coates, *J. Am. Chem. Soc.* **2001**, *123*, 3229.
[52] T. Sakakura, K. Kohno, *Chem. Commun.* **2009**, 1312.
[53] D. J. Darensbourg, S. J. Lewis, J. L. Rodgers, J. C. Yarbrough, *Inorg. Chem.* **2003**, *42*, 581.
[54] Y.-M. Shen, W.-L. Duan, M. Shi, *J. Org. Chem.* **2003**, *68*, 1559.
[55] F. Li, L. Xiao, C. Xia, B. Hu, *Tetrahedron Lett.* **2004**, *45*, 8307.
[56] V. Caló, A. Nacci, A. Monopoli, A. Fanizzi, *Org. Lett.* **2002**, *4*, 2561.
[57] J. Sun, J. Ren, S. Zhang, W. Cheng, *Tetrahedron Lett.* **2009**, *50*, 423.
[58] D. J. Darensbourg, J. L. Rodgers, R. M. Mackiewicz, A. L. Phelps, *Catal. Today* **2004**, *98*, 485.
[59] N. Ikpo, S. M. Butt, K. L. Collins, F. M. Kerton, *Organometallics* **2009**, *28*, 837.
[60] M. D. Eelman, J. M. Blacquiere, M. M. Moriarty, D. E. Fogg, *Angew. Chem.* **2008**, *120*, 309; *Angew. Chem. Int. Ed.* **2008**, *47*, 303.
[61] a) *CrystalClear*, Rigaku Corporation, **1999**, CrystalClear Software User's Guide, Molecular Structure Corporation, **2000**; b) J. W. Pflugrath, *Acta Crystallogr., Sect. D* **1999**, *55*, 1718–1725; c) *SHELX97*: G. M. Sheldrick, *Acta Crystallogr., Sect. A* **2008**, *64*, 112; d) *SIR92*: A. Altomare, G. Cascarano, C. Giacovazzo, A. Guagliardi, M. Burla, G. Polidori, M. J. Camalli, *J. Appl. Crystallogr.* **1994**, *27*, 435; e) *DIRDIF99*: P. T. Beurskens, G. Admiraal, G. Beurskens, W. P. Bosman, R. de Gelder, R. Israel, J. M. M. Smits, The DIRDIF-9 9 program system, Technical Report of the Crystallography Laboratory, University of Nijmegen, The Netherlands, **1999**; f) D. T. Cromer, J. T. Waber, *International Tables for X-ray Crystallography*, vol. IV, The Kynoch Press, Birmingham, England, Table 2.2A, **1974**; g) J. A. Ibers, W. C. Hamilton, *Acta Crystallogr.* **1964**, *17*, 781; h) D. C. Creagh, W. J. McAuley, *International Tables for Crystallography*, vol. C (Eds.: A. J. C. Wilson), Kluwer Academic Publishers, Boston, **1992**, Table 4.2.6.8, p. 219–222; i) D. C. Creagh, J. H. Hubbell, *International Tables for Crystallography*, vol. C (Eds.: A. J. C. Wilson), Kluwer Academic Publishers, Boston, **1992**, Table 4.2.4.3, p. 200–206; j) *CrystalStructure*, v. 3.7.0, Crystal Structure Analysis Package, Rigaku and Rigaku/MSC, 9009 New Trails Dr., The Woodlands, TX 77381, U.S.A., **2000**–**2005**; k) D. J. Watkin, C. K. Prout, J. R. Carruthers, P. W. Betteridge, CRYSTALS Issue 10, Chemical Crystallography Laboratory, Oxford, UK, **1996**; l) A. L. Spek, *J. Appl. Crystallogr.* **2003**, *36*, 7.

Received: July 8, 2011
Published Online: September 16, 2011

